# Core-Shell Nanoscale Ferrite for Thermochemical Hydrogen Generation

V.S. Amar and R.V.Shende*

Department of Chemical and Biological Engineering,
South Dakota School of Mines & Technology,
Rapid City,SD 57701, USA, Rajesh.Shende@sdsmt.edu

## ABSTRACT

In this study, water was used as energy carrier for $H_2$ generation *via* thermochemical water-splitting process using core-shell nanoscale ferrite material, which was synthesized using pluronic P123 templating assisted sol-gel method. Ferrite nanoparticles with porous zirconia shell were thoroughly characterized by powdered x-ray diffraction and BET surface area analyzer. This material was utilized in a continuous flow through tubular reactor as a packed-bed for thermochemical water-splitting process where the regeneration and water-splitting steps were carried out at 1100°C and 900°C, respectively under continuous $N_2$ flow of 35 $cm^3.min^{-1}$ at STP conditions. At these process conditions, five thermochemical cycles were performed. The transient profiles were analyzed to determine the hydrogen volume generation as well as rate of hydrogen generation. Thermochemical water-splitting reactor was integrated with a hydrogen fuel cell to determine the energy conversion. Pressure drop ($\Delta p$) for the packed-bed of Ni-ferrite(c)/$ZrO_2$(s) core-shell nanoparticles was calculated and compared with the packed-bed of Ni-ferrite nanoparticles. In addition, the current output for the hydrogen fuel cell was monitored as a function of hydrogen flow rate.

***Keywords:*** thermochemical water-splitting, hydrogen, core-shell, nanoscale ferrite.

## 1 INTRODUCTION

In a thermochemical water-splitting process [1-3] utilizing redox materials, oxygen and hydrogen are generated in separate steps of regeneration and water-splitting at higher temperatures. In order to make this process feasible at a larger scale, multiple challenges [4-6] need to be addressed, which include efficient heat transfer, material stability, higher temperatures, significant capital cost, corrosion, side-reactions, thermodynamics, reaction kinetics and thermal efficiency. As such nanoparticles have shown higher hydrogen volume generation as compared with micron size particles. Using nanoparticles of redox materials, it has been observed that as number of thermochemical cycles increased, the hydrogen volume decreased [4]. This observation was related to the decrease in surface area upon sintering of the nanoparticles. Consequently, it is imperative to achieve the thermal stabilization of nanoparticles. Very recently, we have attempted to achieve thermal stabilization of Ni-ferrite nanoparticles by encapsulating the nanoparticles inside a thin porous shell of ceramic materials such as $Y_2O_3$ [7] and $ZrO_2$ [8] forming a core-shell morphology.

Novel core-shell nanoparticles of CdS/ZnS [9] were synthesized using the microemulsion technique and used as photocatalysts, which exhibited higher $H_2$ generation rate of 21.2 μmol/h/g from water-splitting under the visible light. ZnO-$TiO_2$ core-shell nanoparticles [10] synthesized *via* atomic layer deposition demonstrated superior photo-electrochemical water-splitting ability and yielded a maximum conversion efficiency of 10%. Although the application of core-shell nanoparticles has been reported in photo-induced reactions, their use in thermochemical water-splitting process has not been fully investigated. Formation of core-shell ferrite nanoparticles with a porous oxide shell is challenging [11] as these particles are magnetic in nature. It may be possible to tune the properties of the porous shell by controlling its chemical composition and porosity by using the surfactant templating approach.

In the case of Ni-ferrite/$Y_2O_3$ core-shell nanoparticles, we have observed relatively stable $H_2$ volume during multiple thermochemical cycles, however, the average $H_2$ volume generation was found to be significantly lower as compared with the Ni-ferrite nanoparticles without the core-shell morphology. This suggests that in the case of core-shell nanoparticles, porous ceramic shell acted as a diffusional barrier for thermochemical reactions which resulted in the mass transfer limitations. We reported [7] these limitations in terms of both external and internal diffusional processes such as: i) gas-film diffusion, ii) gas-solid (shell) interfacial diffusion, iii) diffusion through porous shell layer reaching core-shell interface, and finally, iv) diffusion through the core ferrite material. These diffusional/transport limitations will also exist during the regeneration step. Consequently, both hydrogen and oxygen volume generation and their rates would be expected to be lower for the core-shell nanoparticles. In contrast to this, it is believable that in the case of ferrite nanoparticles, fewer diffusional limitations would exist.

In this study, we have integrated thermochemical water-splitting reactor with a hydrogen fuel cell for energy conversion. A packed-bed of Ni-ferrite (core)/$ZrO_2$ (shell) nanoparticles was used to investigate hydrogen generation wherein we have estimated the porosity and calculated the pressure drop across the bed. In addition, the current output was studied with respect to the hydrogen flow rate.

## 2 EXPERIMENTAL

### 2.1. Synthesis of Core(c)-Shell(s) Ni-ferrite(c)/ $ZrO_2$(s) Nanoparticles

Stoichiometric quantities of chloride based precursor salts of Ni and Fe were taken in ethanol (1:2, wt. ratio) and sonicated until a visually clear solution was obtained. All reagents and precursors were of analytical grade and used as received. Gelation was achieved by the addition of propylene oxide. The resultant gel was aged for 24 hrs and calcined to form Ni-ferrite nanoparticles. Ni-ferrite nanoparticles were suspended in isopropanol with 10 wt.% pluronic P123 surfactant and sonicated in a water bath for 30 min. To this dispersion, previsously calculated Zr-isopropoxide precursor was added dropwise while sonication was in progress. Calcination was carried at 600ºC for 2 hrs. Detailed synthesis method has been reported elsewhere [8].

### 2.2. Characterization of Ni-ferrite(c)/$ZrO_2$(s) Core-Shell Nanoparticles

Sol-gel derived powders receovered after calcination were characterized by the x-ray diffraction using Rigaku Ultima IV X-ray diffractometer (operating conditions- 40 kV, 1.76 kW) in the 2θ range of 10° to 90º. The specific surface area (SSA) and the pore size were determined by using Micromeritics Gemini II – 2375 BET (Brunauer-Emmett-Teller) surface area analyzer. TEM analysis was performed using the JEOL Hitachi H-700 FA transmission electron microscope.

### 2.3. $H_2$ Generation and Energy Conversion

Thermochemical water-splitting reactor set-up for $H_2$ generation was reported in our previous investigation [12]. The core-shell nanopartricles (5 g) were loaded in the Inconel tubular reactor (length- 24 in, inner diameter- 0.85 in) forming a packed bed (Figure 1A), which was supported with ceramic rachig rings. Inconel tubular reactor with the packed-bed of core-shell nanoparticles was enclosed in a high temperature vertical tube furnace. Ultra high purity $N_2$ was used as a carrier gas throughout the thermochemical water-splitting process. During the regeneration step, the Inconel reactor was heated to 1100ºC and held for 2 hours under the constant $N_2$ flow rate of 35 $cm^3.min^{-1}$ at STP conditions. During the subsequent water-splitting step, oxygen deficient ferrite material was exposed to the steam at 900ºC. Oxygen was scavenged by the ferrite material and $H_2$ was released, which was recorded using the online gas sensor (H2SCAN) interfaced with a computer.

The outlet from the $H_2$ sensor was connected to a single-cell proton exchange membrane fuel cell (PEMFC from H-TEC) for energy conversion. Terminals of the fuel cell were connected to the load measurement box (Heliocentris) provided with different resistance from 5 to 200 ohms. Integrated thermochemical water-splitting and fuel cell set-up is schematically shown in Figure 1. Excess $H_2$ rejected from the outlet of the fuel cell was allowed to flare. The current produced under different load conditions was continuously recorded. The purpose of this experiment was to investigate if $H_2/N_2$ product gas can be directly utilized for power generation.

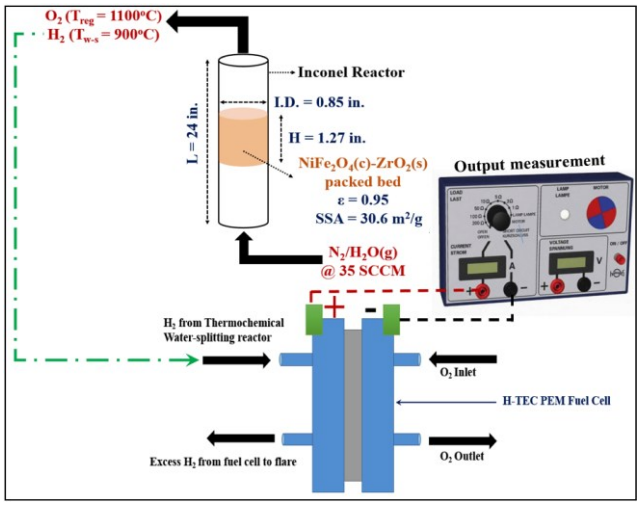


**Figure 1.** Intergrated thermochemical water-splitting and fuel cell set-up for $H_2$ generation and energy conversion.

## 3 RESULTS AND DISCUSSION

### 3.1. Characterization of Core-shell Nanoparticles

Core-shell Ni-ferrite(c)/$ZrO_2$(s) nanoparticles were characterized by powdered x-ray diffraction and the profile obtained is shown in Figure 2. The 2θ reflections indicated

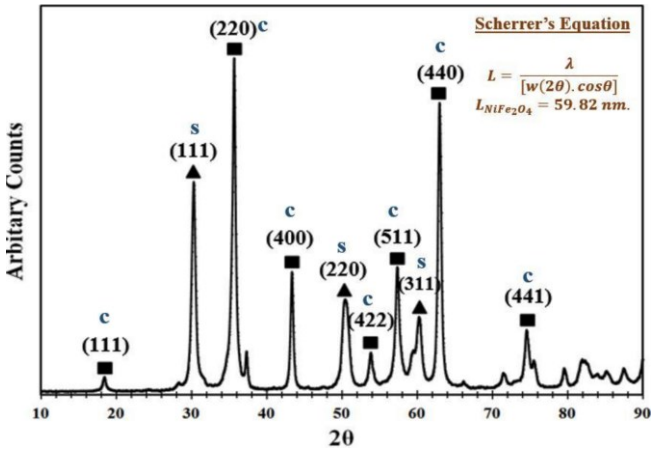


**Figure 2.** X-ray diffraction pattern of calcined Ni-ferrite(c)/ $ZrO_2$(s) core-shell nanoparticles prepared by pluronic 123 surfactant templating assisted sol-gel method.

nominally phase pure $NiFe_2O_4$(c), which is consistent with those reported in the literature [13]. In our earlier study [8], we have reported X-ray diffraction pattern of Ni-ferrite/$ZrO_2$ core-shell nanoparticles, however, Miller indices (*hkl*) were not reported. Three characteristic peaks corresponding to lattice planes of <111>, <220>, and <311> confirmed the presence of tetragonal $ZrO_2$(s). From the Scherrer's equation [4], lattice parameter of $NiFe_2O_4$ was calculated as 59.82 nm.

TEM analysis of $NiFe_2O_4$(c)/$ZrO_2$(s) nanoparticles has been reported previously, which indicated core-shell morphology with $ZrO_2$ shell of 6.12 nm thickness [8]. From the BET analysis, the specific surface area (SSA) of the $NiFe_2O_4$(c)/$ZrO_2$(s) core-shell nanoparticles was found to be 30.60 $m^2/g$.

## 3.2. Packed-Bed Characteristics

As synthesized $NiFe_2O_4$(c)/$ZrO_2$(s) core-shell nanoparticles were placed in the Inconel tubular reactor forming a packed-bed (length- 24 inch, inner diameter- 0.85 inch, height- 2 inch) as shown in Figure 1. The porosity (ε) of the packed-bed was estimated on the basis of bulk density of powdered material. Estimated porosity values prior thermochemical processing are presented in Table 1.

**Table 1.** Comparison of the pressure drop across the packed-bed for both $NiFe_2O_4$(c)/$ZrO_2$(s) core-shell nanoparticles and $NiFe_2O_4$ nanoparticles.

| Parameter | Packed-bed | |
|---|---|---|
| | Core-shell Nanoparticles | $NiFe_2O_4$ nanoparticles |
| Length (m) | 0.032 | 0.051 |
| Diameter (m) | 0.022 | 0.022 |
| ε | 0.51 | 0.78 |
| Δp ($N.m^{-2}/m$) | 1787.76 | 212.88 |
| Δp ($N.m^{-2}$) | 57.60 | 10.81 |

Ergun equation was used to calculate the pressure drop across the packed-bed of $NiFe_2O_4$(c)/$ZrO_2$(s) core-shell nanoparticles, which was compared with that of $NiFe_2O_4$ nanoparticles (Table 1). For calculation purpose, density and viscosity values of $N_2$ carrier gas were considered at the regeneration temperature of 1100°C [15]. Our findings indicate that the presure drop in packed-bed of core-shell nanoparticles is higher than that of packed-bed of $NiFe_2O_4$ nanoparticles. However, as the thermochemical reaction proceeds, grain growth in the $NiFe_2O_4$ nanoparticles will occur due to sintering, which will significantly increase the pressure drop as compared with the packed-bed of core-shell nanoparticles. In the case of core-shell nanoparticles, however, less sintering was observed (data not included).

## 3.3. $H_2$ Generation and Energy Conversion

$H_2$ generation ability of $NiFe_2O_4$(c)/$ZrO_2$(s) core-shell nanoparticles was determined by performing five thermochemical cycles at 900°-1100°C, and compared with the $NiFe_2O_4$ nanoparticles. The transient profiles obtained during several consecutive thermochemical cycles were repoerted in our earlier investigation [8]. Total volume and rate of $H_2$ generation are summarized in Table 2.

**Table 2.** Rate and volume of $H_2$ generation at STP conditions using $NiFe_2O_4$(c)/$ZrO_2$(s) core-shell nanoparticles.

| Cycle No. | $H_2$ Volume at STP (mL) | Rate of $H_2$ Generation ($mL.min^{-1}$) |
|---|---|---|
| 1 | 15.25 | 0.348 |
| 2 | 14.85 | 0.324 |
| 3 | 15.05 | 0.261 |
| 4 | 11.70 | 0.231 |
| 5 | 13.80 | 0.264 |
| Regeneration temp. 1100°C, Water-splitting temp. 900°C | | |

No significant difference was noticed for the rate ($mL.min^{-1}$) and volume of $H_2$ generation observed during five thermochemical cycles performed at the water-splitting and regeneration temperatures of 900°C and 1100°C, respectively using the core-shell nanoparticles. Previously, we have reported $H_2$ volume generation using $NiFe_2O_4$ nanoparticles at identical temperature conditions [7], however, significant reduction in $H_2$ volume was observed during five thermochemical cycles. It suggests that porous $ZrO_2$ shell on $NiFe_2O_4$ nanoparticles has led to partial thermal stabilization and prevented sintering. However, thermal stabilization of the ferrite nanoparticles comes with an expense of lower average $H_2$ yield (2.83 mL/g) as compared with the $NiFe_2O_4$ nanoparticles (avg. $H_2$ yield-28.92 mL/g). It further suggests that diffusional and mass transport limitations exist in core-shell nanoparticles.

Hydrogen produced during thermochemical water-splitting process was directly interfaced to a hydrogen fuel cell for energy conversion. Different load conditions were employed and power output was monitored during five thermochemical cycles. Current outpurt as a function of cumulative hydrogen volume is shown in Figure 3.

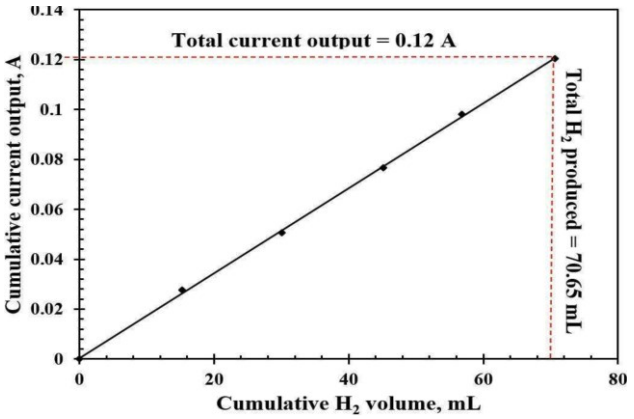


**Figure 3.** Fuel cell current output as a function of cumulative $H_2$ volume generated during five thermochemical cycles performed at water-splitting temperature of 900°C.

Total current output of 0.12 amp was observed corresponding to the cumulative $H_2$ volume of 70.65 mL during five thermochemical cycles. The current produced at a particular load condition was found to be linearly proportional to the $H_2$ flow rate generated per cycle.

## 4 CONCLUSIONS

$NiFe_2O_4(c)/ZrO_2(s)$ core-shell nanoparticles yielded an avg. hydrogen volume 14.15 mL with avg. rate of production of 0.286 $mL.min^{-1}$ in five thermochemical cycles performed at water-splitting temperature of 900°C. Although similar hydrogen volume generation was observed during five thermochemical cycles for the core-shell nanoparticles, it was found to be an order magnitude lower as compared with the hydrogen volume generated using the Ni-ferrite nanoparticles without the core-shell morphology. This indicates the presence of diffusional and mass transfer limitations associated with the core-shell nanopaticles during the thermochemical reaction. Cumulative current output of 0.12 amp was observed for total $H_2$ volume of 70.65 mL during five thermochemical cycles.

## ACKNOWLEDGEMENTS

The authors thankfully acknowledge the financial support from the National Science Foundation, Grant No. CBET#1134570 and Chemical and Biological Engineering department at South Dakota School of Mines & Technology.

## REFERENCES

[1] Funk, J. E., "Thermochemical production of hydrogen via multistage water splitting processes." International Journal of Hydrogen Energy, 1(1), 33-43, 1976.

[2] Fresno, Fernando, Rocio Fernandez-Saavedra, and Manuel Romero, "Solar hydrogen production by two-step thermochemical cycles." International Journal of Hydrogen Energy, 34(7), 2918-2924, 2009.

[3] Nakamura, T., "Hydrogen production from water utilizing solar heat at high temperatures." Solar Energy, 19(5), 467-475, 1977.

[4] Vinod Amar, S., "Hydrogen generation from thermochemical water-splitting process using thermally stabilized redox materials." Ph.D. dissertation, South Dakota School of Mines and Technology, 2016.

[5] Abbasi, Tasneem, and S. A. Abbasi. "Renewable hydrogen: prospects and challenges." Renewable and Sustainable Energy Reviews, 15(6), 3034-3040, 2011.

[6] Offerman, S. E., N. H. Van Dijk, J. Sietsma, S. Grigull, E. M. Lauridsen, L. Margulies, H. F. Poulsen, M. Th Rekveldt, and S. Van der Zwaag, "Grain nucleation and growth during phase transformations." Science, 298(5595), 1003-1005, 2002.

[7] Amar, V. S., Puszynski, J. A., & Shende, R. V., "$H_2$ generation from thermochemical water-splitting using yttria stabilized $NiFe_2O_4$ core-shell nanoparticles." Journal of Renewable and Sustainable Energy, 7(2), 023113, 2015

[8] Amar, V. S., Puszynski, J. A., & Shende, R. V., "Hydrogen generation from thermochemical water-splitting using core-shell Ni-ferrite nanoparticles." Cleantech Proceedings, 139-142, 2014.

[9] Li, Yabin, Zhifeng Liu, Yun Wang, Zhichao Liu, Jianhua Han, and Jing Ya, "$ZnO/CuInS_2$ core/shell heterojunction nanoarray for photoelectrochemical water splitting." International Journal of Hydrogen Energy 37(20), 5029-15037, 2012.

[10] Liu, Mingzhao, Chang-Yong Nam, Charles T. Black, Jovan Kamcev, and Lihua Zhang, "Enhancing water splitting activity and chemical stability of zinc oxide nanowire photoanodes with ultrathin titania shells." The Journal of Physical Chemistry C, 117(26), 13396-13402, 2013.

[11] Ghosh Chaudhuri, Rajib, and Santanu Paria, "Core/shell nanoparticles: classes, properties, synthesis mechanisms, characterization, and applications." Chemical reviews, 112(4), 2373-2433, 2011.

[12] Amar, Vinod S., Xavier M. Pasala, Jan A. Puszynski, and Rajesh V. Shende, "Sonication derived powdered mixtures of ferrite and ceramic nanoparticles for $H_2$ generation." American Journal of Energy Research, 3(2), 25-31, 2015.

[13] Yu, Byong Yong, and Seung-Yeop Kwak, "Self-assembled mesoporous Co and Ni-ferrite spherical clusters consisting of spinel nanocrystals prepared using a template-free approach." Dalton Transactions, 40(39), 9989-9998, 2011.

[14] Ergun, Sabri, and Orning Ao Ao, "Fluid flow through randomly packed columns and fluidized beds." Industrial & Engineering Chemistry, 41(6), 1179-1184, 1949.

[15] McLinden, M. O., "Thermophysical properties of fluid systems." NIST, 1997.